

# Performance of a Miniature, Cold-Cycle Dilution Refrigerator at Tilt Angles between 0 and 30 Degrees

R. Snodgrass, J. Ullom, and S. Backhaus

National Institute of Standards and Technology, Boulder, CO 80305  
Department of Physics, University of Colorado Boulder, Boulder, CO 80309

## ABSTRACT

Cold-cycle dilution refrigerators (DRs) recirculate  $^3\text{He}$  from the still via condensation on a cooled surface; condensate from the cooled surface returns toward the mixing chamber via gravity. Compact versions of these DRs are being considered for astrophysics balloon missions, but it is uncertain if they can provide sufficient temperature stability and if they are able to operate when tilted. Here, we show that a cold-cycle DR from Chase Research Cryogenics can successfully cool to about 70 mK at tilt angles up to and including  $30^\circ$ . There is a persistent change in the temperature of the mixing chamber when tilted, but the variation is only  $\pm 5$  mK between  $0^\circ$  and  $30^\circ$ . However, we have also identified that tilting at some azimuthal angles can interrupt the cooling process at the mixing chamber, perhaps by the translation of the fluid interfaces within the DR. Interrupted cooling at the mixing chamber can be avoided by mounting the DR in the proper azimuthal orientation relative to the tilt axis. We also show that  $10 \mu\text{K}$  RMS temperature stability can be achieved at the mixing chamber while continuously tilting the DR at  $6^\circ/\text{h}$ . This stability is only achieved over 89% duty cycle because of large, cyclical perturbations to temperature that originate in the DR's  $^3\text{He}$ - $^4\text{He}$  adsorption pre-cooler. Temperature perturbations to the  $^3\text{He}$  condenser are cascaded to every other component of the DR, likely by heat advection through the unconstrained concentrated and dilute liquid columns.

## INTRODUCTION

Cold-cycle dilution refrigerators (DRs) are a potential alternative to adiabatic demagnetization refrigerators (ADRs) for the cooling of X-ray and  $\gamma$ -ray detectors aboard balloon missions. These DRs can be very small (the DR discussed here has a cylindrical footprint of 17 cm diameter and 26 cm height), do not require magnetic shielding for sensitive detectors (as is the case for ADRs), and operate with a 4.2 K stage cooled by a liquid  $^4\text{He}$  bath or cryocooler. Besides precooling, the only other requirement for these DRs is an array of heaters to cycle adsorption pumps and heat switches. With automation, they cool continuously to mK temperatures.

Cold-cycle DRs can be so compact because  $^3\text{He}$  is circulated without the assistance of room temperature gas handling systems. Instead, the dilution unit is permanently sealed and  $^3\text{He}$  from the still is condensed onto a cold surface and flows back down towards the mixing chamber via gravity. This type of dilution refrigerator was first implemented by Edel'man [1], but has been developed more-recently by Mikheev et al. [2] and Teleberg et al. [3]. The condenser of the DR

studied here is continuously cooled to around 400 or 500 mK using four adsorption-pumped helium evaporators. Two of the evaporators are  $^4\text{He}$  and are used to cool two  $^3\text{He}$  evaporators. Each  $^3\text{He}$ - $^4\text{He}$  pair runs in antiphase to achieve continuous cooling of the DR's condenser.

The focus of this study is the performance of a cold-cycle DR at different tilt angles – an important topic because  $^3\text{He}$  recirculation relies upon gravity and because these DRs are being considered for balloon missions where the cryostat may be tilted continuously throughout flight to track objects in the sky. All results are from a DR purchased from Chase Research Cryogenics (CRC)<sup>1</sup>. We show that the dilution refrigerator can operate well at tilt angles between  $0^\circ$  and  $30^\circ$ , but that at certain azimuthal angles the tilted dilution refrigerator may fail; this failure can be easily avoided by mounting the DR in the correct azimuthal orientation before flight. We also show that temperature perturbations to the mixing chamber may arise from advection of the liquids on the concentrated and dilute sides of the mixing chamber. The mixing chamber achieves good temperature stability at up to 89% duty cycle even while being continuously tilted.

## EXPERIMENTAL METHODS

Figure 1 shows a schematic of the Chase Research Cryogenics (CRC) miniature, cold-cycle dilution refrigerator. The left shows the evaporative pre-cooler while the right shows the dilution refrigerator; the two are mounted tightly together. The function of the pre-cooler is to keep the  $^3\text{He}$  condenser of the DR cooled continuously to nearly the temperature of the active  $^3\text{He}$  adsorption refrigerator(s). The pre-cooler was itself cooled by a two-stage, 1.4 Hz commercial pulse tube refrigerator. The main plate of the pre-cooler was sometimes regulated to 4.2 K to simulate a liquid  $^4\text{He}$  bath, and at other times left unregulated. When left unregulated, the main plate spent much of the pre-cooling cycle between 2.5 K and 3 K: this produced mixing chamber temperatures that were about 1.5 mK colder than if the main plate was regulated to 4.2 K.

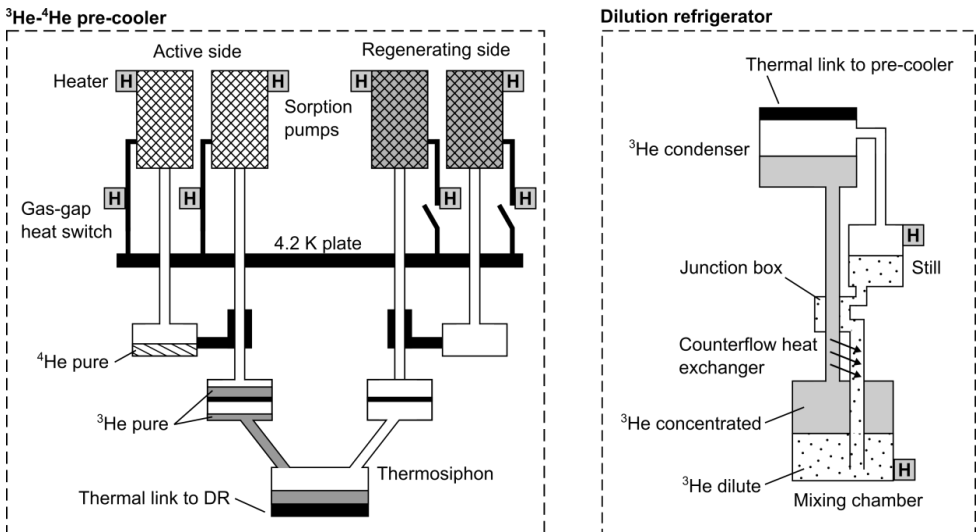


**Figure 1.** Schematic of the pre-cooler (left) and dilution refrigerator (right). The active side of the pre-cooler is shown during the part of the cycle where the heat switches are closed and most of the helium is in the pots – the pumps have recently been cooled by the main plate and are beginning to adsorb helium, cooling the pots. The regenerating side is shown at the stage where all the helium from the pots has been adsorbed in the pumps, so the heat switches have recently been opened and the pumps are ready to be heated, which will release the helium back to the pots. The junction box in the DR is used to separate the concentrated and dilute lines of the counterflow heat exchanger. Black shapes in this figure are those with strong thermal conduction.

<sup>1</sup> Certain commercial products are identified to specify the experimental study adequately. This does not imply endorsement by NIST or that the products are the best available for the purpose.

The pre-cooler achieves continuous cooling of the DR’s condenser by implementation of two, identical <sup>3</sup>He-<sup>4</sup>He adsorption refrigerators that operate in antiphase from each other. While one side contains liquid helium and is cooling via evaporation to the charcoal pumps (the active side), the other side is in the process of regeneration by heating the charcoal pumps, releasing the adsorbed helium, and re-condensing it into the <sup>4</sup>He and <sup>3</sup>He pots. A gravity-driven heat pipe (thermosiphon) in a split configuration contacts the two <sup>3</sup>He pots. The <sup>3</sup>He in the thermosiphon condenses on the active <sup>3</sup>He pot and is gravity-fed down into a volume that has good thermal contact with the <sup>3</sup>He condenser of the DR unit; the other leg of the thermosiphon has poor thermal contact with the (hot) regenerating <sup>3</sup>He pot, as there is no liquid <sup>3</sup>He in that leg. The thermosiphon therefore acts as a passive pair of heat switches. We have not yet properly characterized the thermosiphon’s performance, although we hope to do so in the future.

The experimental details of operating the <sup>3</sup>He-<sup>4</sup>He pre-cooler are given in Table 1. Heaters on the adsorption pumps and gas-gap heat switches drive the pre-cooling cycle. The heat switches thermally connect (during the active part of the cycle) or disconnect (during regeneration) the adsorption pumps from the main plate cooled by the pulse tube refrigerator. Further description of the pre-cooler is outside the focus of this manuscript, but more information may be found in [4].

The DR itself is similar to traditional ones except in how <sup>3</sup>He is recirculated. A condenser is connected to the still by a small tube that allows for the flow of <sup>3</sup>He vapor. The vapor is condensed on a surface cooled by the thermosiphon and flows towards the mixing chamber using gravity. Heaters are placed on the still and mixing chamber.

A variety of thermometry was placed on the pre-cooler and dilution unit. Pump and heat switch temperatures were measured using standard-curve (i.e., uncalibrated) silicon diodes installed by CRC. Chase Research Cryogenics also installed standard-curve ruthenium oxide (ROX) thermometers on the <sup>3</sup>He and <sup>4</sup>He pots, the <sup>3</sup>He condenser, the still, and the mixing chamber. With the exception of one of the <sup>4</sup>He pots, however, this thermometry was unused; instead, we installed calibrated ROX thermometers at these locations. We self-calibrated these

**Table 1:** Half-cycle pre-cooler procedure.\* After the listed steps are completed, program proceeds to step 1 of the other side. Switch heat values differ between sides because their temperature responses differ (attempted to keep switches at about 18 K when on). A software mistake caused a 10-minute dwell to occur after step 8 for only one of the half-cycles (making the two half-cycles slightly asymmetric). Numbers separated by semicolons are given respectively for <sup>4</sup>He and <sup>3</sup>He. The <sup>3</sup>He pots continue to cool after step 8, i.e., during the half-cycle of the opposite side.

Step	Description	Heat (mW)	Time criteria to advance (min)	Temperature criteria to advance (K)
1	<sup>4</sup> He and <sup>3</sup> He heat switches off	0	8	-
2	Begin to heat <sup>4</sup> He pump and <sup>3</sup> He pump	40; 20	25**	<sup>4</sup> He pot > 1.4; <sup>3</sup> He pot > 1.1
3	Heat <sup>4</sup> He pump and <sup>3</sup> He pump	600 (60^); 330 (33^)	25**	<sup>4</sup> He pump > 45; <sup>3</sup> He pump > 45
4	<sup>4</sup> He pump off	0	10	-
5	<sup>4</sup> He switch on	A side: 2.5 (1.5^) B side: 2.5 (0.75^)	10**	<sup>4</sup> He switch > 18 K
6	Wait for <sup>4</sup> He pot to cool	-	25**	<sup>4</sup> He pot < 0.9 K
7	<sup>3</sup> He pump off	0	0	-
8	<sup>3</sup> He switch on	A side: 2.5 (2^) B side: 2.5 (0.75^)	10**	<sup>3</sup> He switch > 18 K

\*Opposite side heat switches remain on for this half-cycle. \*\*If temperature criterion is not met, step advances once this time expires. ^Heat value after the temperature or time criterion is met (persists until turned off in a later step).

ROX thermometers using one calibrated by the thermometry manufacturer. ROX thermometry was read using a Lakeshore 370 AC resistance bridge with preamp/scanner. The excitation level was set to 3.16 nA for all ROX thermometry except for the data shown in Fig. 7, where the excitation of the mixing chamber thermometer was increased to 31.6 nA for increased measurement resolution at the cost of about 2 mK of self-heating.

We also installed two self-calibrated ROX thermometers on the concentrated side (annulus) of the counterflow heat exchanger of the dilution unit. To do so, we made two small, 101 copper split clamps that fit snugly around the (stainless steel) outer heat exchanger tube, applying a thin layer of thermal grease to improve the thermal contact between clamp and tube. These thermometers were placed roughly 2% and 12% along the length of the heat exchanger (where 0% is the condenser and 100% is the mixing chamber). For a single experiment, we also placed one of these copper split clamps on the dilute line flowing from the junction box to the still, measuring just a few mK below the temperature of the condenser (data not shown). From this observation, we gather that the dilute liquid from the counterflow heat exchanger makes excellent thermal contact with the condenser before proceeding to the still, and that the dilute mixture enters the still at a temperature very close to the temperature of the condenser.

## RESULTS AND ANALYSIS

### $^3\text{He}$ flow rate through the dilution refrigerator

Before proceeding to the performance of the DR at different tilt angles, we discuss how the temperature perturbations originating in the condenser reach the mixing chamber. This is an

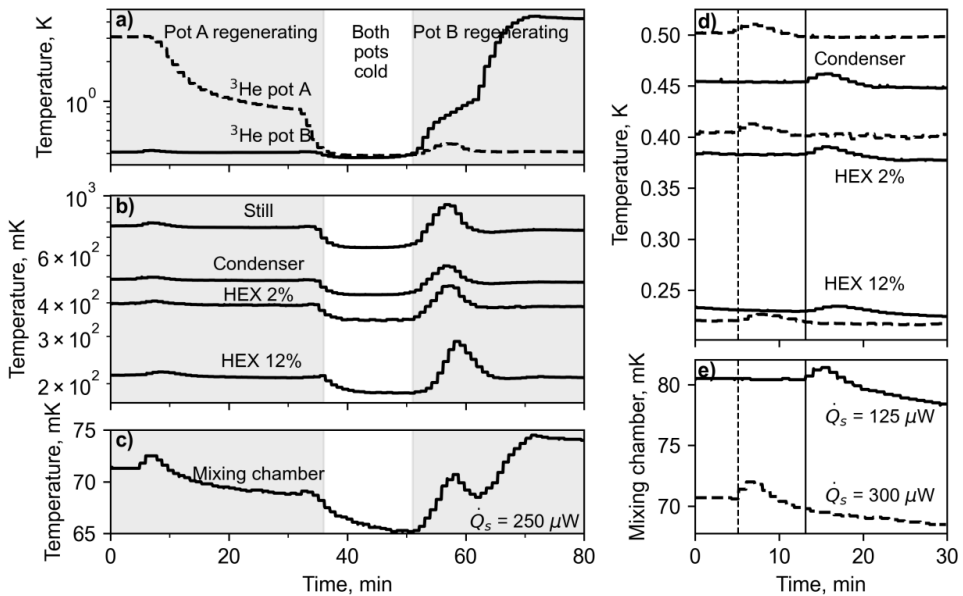


**Figure 2.** Typical dilution refrigerator temperatures during the transition between which  $^3\text{He}$  pot cools the condenser. In the left shaded region, pot B is cooling the condenser, while in the right shaded region, pot A is cooling the condenser. At the beginning of regeneration (just past 50 minutes), the temperature of the condenser rises with the regenerating pot, showing that there is a heat leak from the regenerating leg of the thermosiphon. a) The  $^3\text{He}$  pot temperatures. b) The temperatures of the DR components excluding the mixing chamber. HEX 2% and 12% are the readings from thermometers placed 2% and 12% along the length of the counterflow heat exchanger (concentrated side). c) The temperature of the mixing chamber. Subplots d) and e) also show the perturbations that occur when the regenerating  $^3\text{He}$  pot becomes cold but are from two different experiments where the still heat was set to  $125\ \mu\text{W}$  (solid lines) or  $300\ \mu\text{W}$  (dashed lines). Vertical lines are a visual guide to show the beginning of each temperature perturbation.

important topic because it builds understanding of the important physical processes within the DR and because temperature stability at the mixing chamber is critical for the cooling of detectors.

The largest temperature perturbations to the mixing chamber occur when there is a change in heat transfer between the  $^3\text{He}$  pots and the thermosiphon; this occurs when the  $^3\text{He}$  pots change from active to regenerating, or vice-versa (Fig. 2a-c). As the regenerating pot is cooled the temperature of the condenser drops from about 485 mK to 430 mK. At this point, both pots cool the condenser and any heat leak from the dry leg of the split thermosiphon is removed. Figure 2 shows that not just the condenser, but all components of the DR decrease in temperature at nearly the same time. Thermometry at the DR components was sampled at about 1-minute increments, and the temperature perturbations originating in the condenser are seen throughout the whole DR on a similar timescale.

Now we consider if temperature perturbations at the condenser could migrate to the mixing chamber at the timescale observed in Fig. 2a-c simply through the steady  $^3\text{He}$  flow rate  $\dot{n}$ . To estimate  $\dot{n}$  we perform a First Law balance at the still, considering only  $^3\text{He}$  since we will assume that no (or little)  $^4\text{He}$  is circulated. The still heat  $\dot{Q}_s$  is balanced by the latent heat of vaporization  $L_3$  of the  $^3\text{He}$  and the cooling provided by the cold, dilute  $^3\text{He}$  mixture entering the still from the junction box (at the temperature of the condenser):

$$\dot{Q}_s = \dot{n}[L_{3,s}(T_m) + h_{3,s}(T_m) - h_{3,3}(T_m)], \quad (1)$$

where  $h_3$  is the molar enthalpy of  $^3\text{He}$  in mixture with  $^4\text{He}$ . The second number in the subscript of  $L_3$  and  $h_3$  denotes evaluation at  $T_3$  or  $T_s$  (the temperature of the  $^3\text{He}$  condenser and still, respectively). Note that the latent heat and enthalpy in Eq. (1) are dependent upon the mixing chamber temperature  $T_m$  because  $T_m$  determines the  $^3\text{He}$  concentration throughout the dilute line [5]. Also note that  $h_{3,3}$  is evaluated for the dilute mixture but at the temperature of the condenser because that is the temperature of the liquid entering the still. For this estimate, we will set  $T_m = 0.1$  K,  $T_s = 0.75$  K, and  $T_3 = 0.5$  K. We calculate  $h_{3,s} - h_{3,3}$  as  $\int_{T_3}^{T_s} c dT$ , where  $c$  is the specific heat of liquid  $^3\text{He}$  in mixture with  $^4\text{He}$  (also dependent upon  $T_m$ ). Using Fig. 18 and Fig. 20 from [5], we estimate  $h_{3,s} - h_{3,3}$  as 5.3 J/mol and  $L_{3,s}$  as 24.7 J/mol. Rearranging the above equation for  $\dot{n}$  and using  $\dot{Q}_s = 250$   $\mu\text{W}$ , we estimate  $\dot{n}$  as 8  $\mu\text{mol/s}$ .

Using the density of liquid  $^3\text{He}$  (0.082 g/cm<sup>3</sup> [6]), we estimate the volume flow rate of  $^3\text{He}$  through the DR as  $2.9 \times 10^{-10}$  m<sup>3</sup>/s. Although we do not know the design details of the counterflow heat exchanger besides that the concentrated liquid flows through the annulus, we will assume that it is a simple, tube-in-tube design where the annulus has a cross-sectional area of 1 mm<sup>2</sup>. We estimate its length as 71 cm. Using this geometry and our estimated flow rate, it takes approximately 41 minutes for a  $^3\text{He}$  atom to flow from the beginning of the counterflow heat exchanger (concentrated side) to the entrance of the mixing chamber. Therefore, the flow of  $^3\text{He}$  through the system by the dilution process alone cannot explain the rapid propagation of temperatures perturbations through the DR.

This conclusion is further supported by the experiments shown in Fig. 2d-e, where we analyzed the propagation of the temperature perturbation at a variety of still heats. Even for a still heat of 125  $\mu\text{W}$  (which should decrease the  $^3\text{He}$  flow rate from about 8  $\mu\text{mol/s}$  to 4  $\mu\text{mol/s}$ ) the perturbation from the condenser was observed nearly instantaneously on the mixing chamber and heat exchanger thermometers.

### Advection in the dilution refrigerator and U-tube simplification

We believe the rapid propagation of temperature perturbations through the DR stems from moving liquid columns in the dilution refrigerator. The liquid surfaces in the condenser, still, and mixing chamber are not fixed in space but can translate up and down, resulting in the advection of heat.

The liquids in the DR may be thought of as two sides of a U-tube (Fig. 3 side view). One side of the U-tube is occupied by the less-dense, concentrated liquid, while the other side is occupied

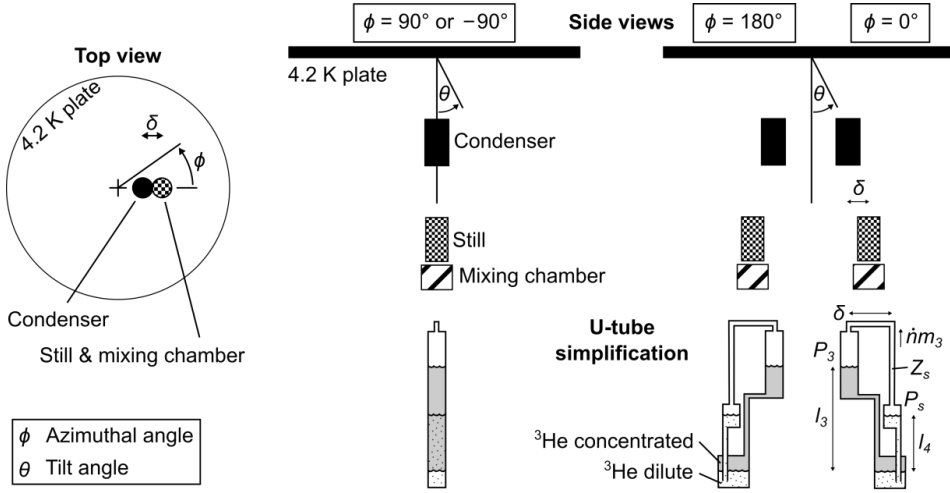


**Figure 3.** (Left) A top view of the critical components of the dilution refrigerator. (Right) The same components shown in side views perpendicular to the tilt axis. For azimuthal angles  $\phi$  not equal to  $90^\circ$  or  $-90^\circ$ , a horizontal offset  $\delta$  exists between the condenser and the still and mixing chamber. The horizontal offset is maximum for  $\phi = 0^\circ$  and  $180^\circ$ . The vapor pressure above the condenser is  $P_3$ , while the vapor pressure above the still is  $P_s$ .

by the more-dense, dilute mixture. The two legs of the U-tube are connected by the vapor space between the condenser and still. If there are no dead volumes where liquid may become trapped and assuming fixed volumes of concentrated and dilute liquids, a drop in the surface of the concentrated liquid column requires a drop in the phase boundary in the mixing chamber and a rise of the dilute surface in the still (and vice versa).

The height of the liquid surfaces is determined by the hydrostatic pressures and the viscous pressure drop across the still line. A closed path integral of pressure changes  $dp$  using path coordinate  $s$  starting at the phase boundary in the mixing chamber and proceeding in the direction of the still, then traversing through the still-condenser tube, and finally returning to the mixing chamber through the concentrated return line requires:

$$\oint \frac{dp}{ds} = 0 = \rho_4 g l'_4(\theta, \phi) - \frac{\dot{n} m_3}{\rho_3} Z_s - \rho_3 g l'_3(\theta, \phi), \quad (2)$$

where the densities of the mixtures are approximated by  $\rho_4$  and  $\rho_3$  – the densities of liquid  $^4\text{He}$  and  $^3\text{He}$ , respectively,  $g$  is the acceleration due to gravity,  $l'_4$  and  $l'_3$  are the heights of the dilute and concentrated liquids above the phase boundary (their dependence upon tilt angle  $\theta$  and azimuthal angle  $\phi$  will be explained in the following section),  $\rho_3$  is the density of the  $^3\text{He}$  vapor in the still line,  $m_3$  is the molar mass of  $^3\text{He}$ , and  $Z_s$  is the volumetric flow impedance of the still line. We estimate that the flow through the still line is laminar<sup>2</sup>.

For this preliminary analysis we will briefly discuss a few implications of Eq. (2). The first is the connection between still/condenser temperature and the height of the liquid columns. The density of the vapor in the still line  $\rho_3$  depends upon  $T_3$  and  $T_s$ , so changes to the temperature of the still or condenser may result in changes to the viscous pressure drop and corresponding changes to the dilute and concentrated column heights according to Eq. (2).

The above may explain the rapid propagation of temperature perturbations at the condenser through the rest of the DR. For an increase to the viscous pressure drop across the still line there must be an increase to the height of the dilute column and a decrease to the height of the concentrated column. This results in the rapid flow of concentrated  $^3\text{He}$  from the condenser down

<sup>2</sup> Using viscosity from [7], we estimate the Reynolds number in the still line to be between 1 and 10.

the counterflow heat exchanger towards the mixing chamber. This flow does not have enough time to effectively transfer heat with the dilute mixture flowing towards the still, so the  $^3\text{He}$  entering the mixing chamber is warmer than before the perturbation and the mixing chamber warms. At all locations along the concentrated side of the counterflow heat exchanger warmer liquid from above replaces the colder liquid that was previously there, advecting heat. This process could rapidly propagate temperature perturbations, as observed in the measurements of Fig. 2, and will be considered in more detail in a future publication. Changes to  $\dot{n}$  could also fluctuate the liquid columns, but for each of our experiments the still heat was unchanged, so  $\dot{n}$  should be relatively stable for the perturbations to  $T_3$  and  $T_s$ , which were of order 0.1 K.

In Eq. (2) the column heights are written as functions of  $\theta$  and  $\phi$  (this dependence is discussed further in the next section). The orientation of the DR will change the hydrostatic pressures and therefore the pressure drop across the still line. The result is that the still and condenser temperatures may be affected by changing the tilt angle and/or azimuthal angle.

**Azimuthal angle  $\phi$**

The dilution refrigerator and cryostat may be rotated (Fig. 3) around two different axes: a tilt axis (denoted by  $\theta$  and limited between  $0^\circ$  to  $30^\circ$  for our equipment), and an azimuthal axis (denoted by  $\phi$  and limited to  $\pm 180^\circ$ ). Both axes of rotation were automated and controlled by a program written in Python. The cryostat was tilted using a linear actuator and was rotated around the azimuth using a large stepper motor.

When viewed from above (Fig. 3), the  $^3\text{He}$  condenser is horizontally offset from the still and mixing chamber (which are coaxial) by distance  $\delta$ . This horizontal offset makes the liquid column heights in the DR dependent upon the azimuthal angle  $\phi$  when  $\theta \neq 0^\circ$ . For example, when  $\phi = 90^\circ$ , the horizontal offset is eliminated relative to the tilt angle  $\theta$ , and the condenser, still, and mixing chamber are all aligned when viewed from the side. When tilted in this orientation,  $l'_3 = l_3 \cos \theta$  ( $l_3$  is the concentrated column length at no tilt), and  $l'_4 = l_4 \cos \theta$  ( $l_4$  is the dilute column length at no tilt). When tilted at  $\phi = 0^\circ$ , the horizontal offset is at a maximum and

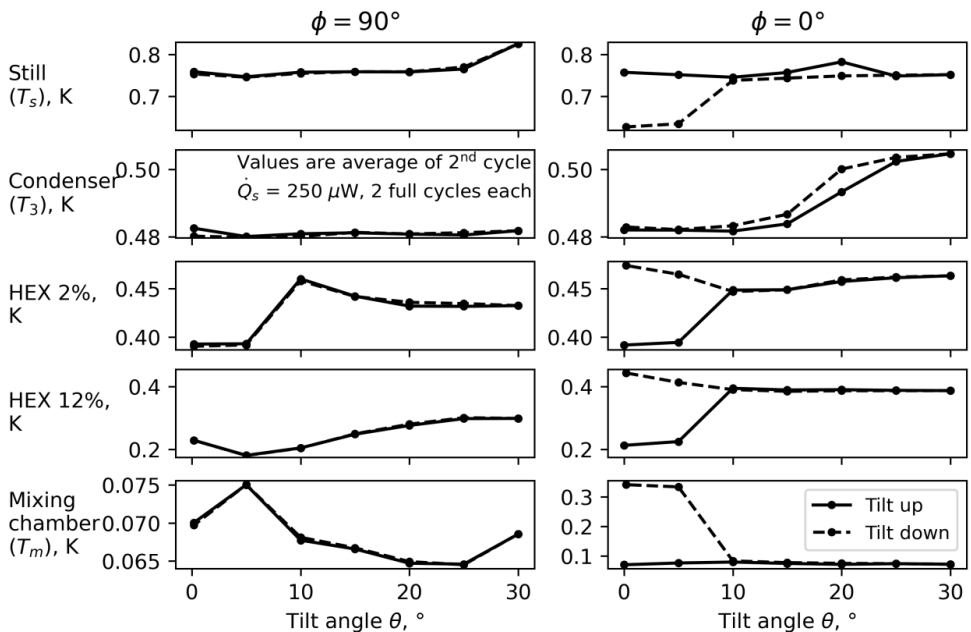


**Figure 4.** Dilution refrigerator temperatures as a function of tilt angle for two different azimuthal orientations ( $\phi = 90^\circ$  in the left column and  $\phi = 0^\circ$  in the right column). Still heat  $\dot{Q}_s$  was fixed at  $250 \mu\text{W}$  for all experiments. Behavior is repeatable for  $\phi = 90^\circ$  but hysteretic for  $\phi = 0^\circ$ .

$l'_3 = l_3 \cos \theta - \delta \sin \theta$ , while  $l'_4 = l_4 \cos \theta$ . The hydrostatic pressure exerted by the two liquid columns is therefore dependent upon  $\phi$ , which may explain some of the performance differences discussed in the following section.

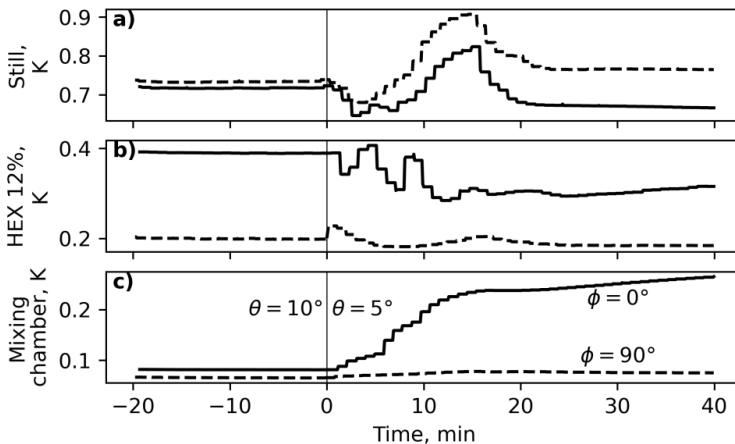
### Performance at different tilt angles $\theta$

Figure 4 summarizes the performance of the DR at tilt angles between  $0^\circ$  and  $30^\circ$ . With the cryostat oriented at  $\phi = 90^\circ$  (left column) and  $\phi = 0^\circ$  (right column), it was tilted from  $0^\circ$  to  $30^\circ$  and then back to  $0^\circ$  in  $5^\circ$  increments. Two full-cycles of the pre-cooler were executed at each tilt setting (the duration of two cycles is about 310 minutes). The results shown in Fig. 4 are the cycle-averaged values of only the second cycle (to remove the transient influence of the first).

With zero horizontal offset between condenser, still, and mixing chamber when viewed from the side ( $\phi = 90^\circ$ , left column), Fig. 4 shows that the DR has satisfactory performance for  $\theta$  up to and including  $30^\circ$ . No hysteresis is observed, i.e., the results for tilting up are nearly equivalent as the results for tilting down. The mean mixing chamber temperature rises to about 75 mK ( $\theta = 5^\circ$ ) from 70 mK ( $\theta = 0^\circ$ ); however, at higher tilt angles the mixing chamber temperature is slightly lower than with no tilt (minimum of about 65 mK at  $\theta = 25^\circ$ ). Tilt did not significantly influence  $T_s$  or  $T_3$  except for  $\theta = 30^\circ$ , where the still temperature increased to 825 mK from about 770 mK ( $\theta = 25^\circ$ ).

With maximum horizontal offset ( $\phi = 0^\circ$ , right column), satisfactory  $T_m$  is achieved while tilting up ( $T_m$  between 70 mK and 79 mK), but in the transition from  $\theta = 10^\circ$  to  $\theta = 5^\circ$   $T_m$  suddenly increases from about 83 mK to 330 mK. The dynamics of this process are shown in detail in Fig. 5: immediately after changing  $\theta$  to  $5^\circ$  (that movement was completed in about 5 s),  $T_m$  rapidly increases. The mixing chamber remains near 330 mK after  $\theta$  is decreased from  $5^\circ$  to  $0^\circ$ . Figure 3 also shows that  $T_s$  drops significantly when  $T_m$  rises in temperature. Although  $T_m$  is relatively stable while tilting up,  $T_3$  rises by about 20 mK between  $\theta = 0^\circ$  to  $\theta = 30^\circ$  (this is not observed when  $\phi = 90^\circ$ ). Heat exchanger temperatures are also plotted in Fig. 4 and may be useful in diagnosing the change in liquid levels that may occur when the cryostat is tilted. For example, a significant increase in the heat exchanger temperatures occurs in the transition from  $\theta = 5^\circ$  to  $\theta = 10^\circ$  (i.e., tilting up), which suggests a change in liquid surfaces.

The run-away  $T_m$  behavior for  $\phi = 0^\circ$  is repeatable. We performed the same experiment but with  $T_m$  regulated to 85 mK (data not shown), and  $T_m$  suddenly increased to about 340 mK after



**Figure 5.** Dynamic detail of the mixing chamber temperature run-away when  $\phi = 0^\circ$  (solid lines), with  $\phi = 90^\circ$  (dashed lines) for comparison. Transition from  $10^\circ$  to  $5^\circ$  tilt occurs at 0 minutes. The temperature at 12% down the heat exchanger (concentrated side) is near 0.2 K or 0.3 K (repeatable for tilt-up versus tilt-down) when  $\phi = 90^\circ$ ; however, for  $\phi = 0^\circ$  that temperature increases from 0.2 K to about 0.4 K rapidly after the transition from  $5^\circ$  tilt to  $10^\circ$  tilt and remains near that elevated temperature for all tilt angles, as shown in Fig. 4.



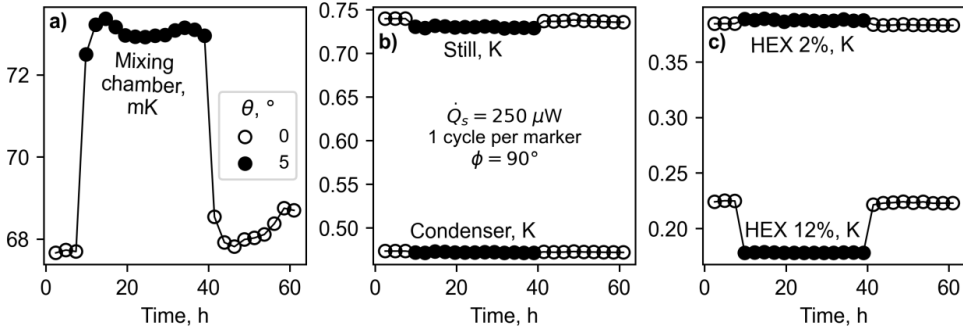


**Figure 6.** Dilution refrigerator temperatures when tilted from  $0^\circ$  to  $5^\circ$  and allowed to stabilize for 13 cycles (about 32 hours). Each marker corresponds to one full cycle of the pre-cooler.

the transition from  $\theta = 10^\circ$  to  $\theta = 5^\circ$ . Furthermore, the dilution process does not seem to recover after the run-away. We observed  $T_m$  near 340 mK for over 16 h with no sign of changing. We were able to eventually reset the dilution process by heating the DR to about 1 K and allowing it to cool again. The same experiment has also been performed for  $\phi = 180^\circ$  ( $T_m$  regulated to 85 mK). At this orientation,  $T_m$  does not rise to  $> 300$  mK, but to about 90 mK, so performance is still severely hindered for  $\phi = 180^\circ$ . Although we have not yet fully explained the markedly different behavior for  $\phi = 0^\circ$  (unstable),  $\phi = 180^\circ$  (stable but poor performance) and  $\phi = 90^\circ$  (stable with good performance), we do believe that the  $\phi$ -dependence on  $l'_4$  and  $l'_3$  (see previous section) may be responsible (or may exacerbate a phenomenon that occurs at all  $\phi$ ).

**Influence of tilt is persistent**

Advection has previously been discussed as a mechanism for rapid temperature change in the dilution unit. For example, a change in  $\theta$  may result in translation of the liquid columns (through  $l'_4$  and  $l'_3$  in Eq. (2)) that in-turn change  $T_m$ . However, the effects of advection may be transient, and other mechanisms with longer timescales (such as the process of  $^3\text{He}$  atoms making a complete loop around the DR) may also be responsible for the trends presented in Fig. 4.

To test whether the influence of tilt is transient or steady, we completed many pre-cooler cycles at two different  $\theta$  (Fig. 6). First, three cycles were completed at  $\theta = 0^\circ$ , then thirteen cycles

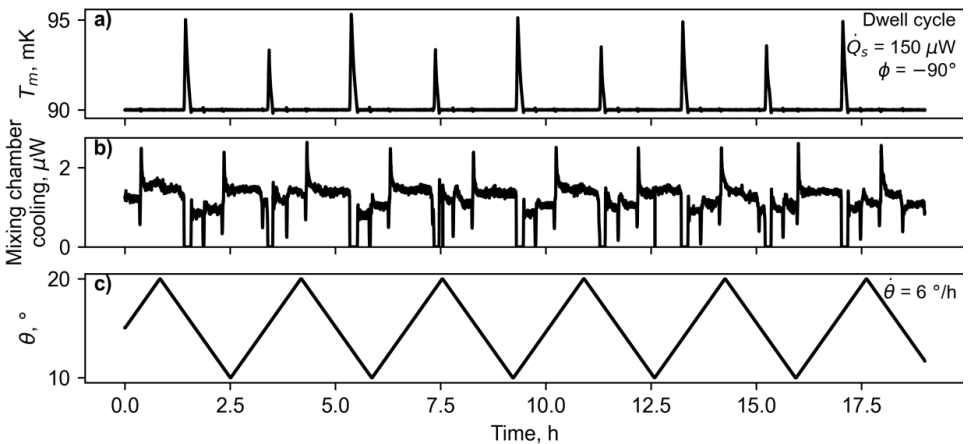


**Figure 7.** Regulation of the mixing chamber at 90 mK while tilting continuously between  $10^\circ$  and  $20^\circ$  at  $6^\circ/\text{h}$ . a) Mixing chamber temperature. The large spikes (of size  $\sim 5$  mK) occur when the active  $^3\text{He}$  pot begins to heat (regenerate). Two smaller deviations from 90 mK (of size  $\sim 0.1$  mK) are difficult to make out but occur when the heat switches between hot adsorption pump and cold main plate are turned on. b) Cooling power of the mixing chamber at 90 mK. c) The tilt angle  $\theta$ .

(about 32 h) were completed at  $\theta = 5^\circ$ , and lastly the cryostat was tilted back down to  $0^\circ$  for nine more cycles. No temperatures in the dilution refrigerator seemed to significantly change within each tilt setting, i.e., all temperatures in the DR appeared to depend on  $\theta$  but not time. We conclude that tilt has a persistent change on the performance of this dilution refrigerator.

### Mixing chamber temperature stability while tilting

This miniature dilution refrigerator will be flown on a balloon mission to cool microcalorimeters. Besides cooling to about 80 mK or 90 mK, temperature stability is of utmost importance for sensor operation. Furthermore, it is desirable that the entire cryostat (including DR and detectors) is able to continuously tilt so that objects in the sky may be tracked.

Figure 7 displays the temperature of the mixing chamber when regulated to 90 mK while continuously tilting the cryostat between  $10^\circ$  and  $20^\circ$  at a tilt rate of  $6^\circ/\text{h}$ . During these experiments  $\phi$  was set to  $-90^\circ$  (which, like  $\phi = 90^\circ$ , is stable) and the still heat was set to  $150 \mu\text{W}$ . Additionally, the cycle described in Table 1 was slightly modified. The most critical change to the pre-cooler cycle was that a 60-minute dwell was implemented during the time that both  $^3\text{He}$  pots are cold (i.e., the unshaded region of Fig. 2). Such a long dwell time was made possible by the relatively low still heat, which minimized the  $^3\text{He}$  flow rate and heat load on the pre-cooler.

With the changes to the cycle procedure and still heat,  $T_m$  was regulated to 90 mK over an 89% duty cycle. Over this 89% duty cycle the temperature stability of the mixing chamber was measured to be  $10 \mu\text{K}$  RMS (using a 1 s hardware filter). Slightly higher duty cycles may be achieved by increasing the dwell time, although that would require lower  $^3\text{He}$  flow rates (and therefore higher mixing chamber temperatures). We were unable to remove the large spikes in  $T_m$  shown in Fig. 7a by temperature regulation of the mixing chamber – these large perturbations occur when the previously active  $^3\text{He}$  pot begins its regeneration process (Fig. 2 shows detail of these dynamics).

## CONCLUSION

The Chase Research Cryogenics miniature, cold-cycle dilution refrigerator can achieve continuous cooling to about 70 mK (mean, no load) at tilt angles up to at least  $30^\circ$ . We recommend mounting the DR in cryostats so that the condenser, still, and mixing chamber are all colinear with one another when viewed from the side at an angle perpendicular to the tilt axis ( $\phi = 90^\circ, -90^\circ$  by our convention). Under this condition, we found a small, yet persistent influence of tilt angle on mixing chamber temperature ( $\pm 5 \text{ mK}$  from the temperature at no tilt). We identified other, undesirable orientations ( $\phi = 0^\circ$ ) where the mixing chamber can heat to  $> 300 \text{ mK}$  after tilting to  $30^\circ$  and then back towards  $0^\circ$ . When this mixing chamber temperature run-away occurs, it does not recover until the dilution unit is heated and allowed to cool again (this likely resets the surfaces of the concentrated and dilute liquids).

Temperature stability of the mixing chamber was measured as  $10 \mu\text{K}$  RMS over an 89% duty cycle even while tilting the DR at  $6^\circ/\text{h}$ . This is a promising result for the DR's feasibility as a cooler aboard balloon missions or for other, terrestrial applications where continuous tilting of a cryostat is necessary. We judge it unlikely that much higher duty cycles can be achieved, as a relatively large heat load is placed on the  $^3\text{He}$  condenser when the previously active  $^3\text{He}$  pot of the pre-cooler begins to regenerate. This causes the condenser to rise in temperature, and perturbations to the condenser are transmitted nearly instantaneously throughout the dilution refrigerator (including mixing chamber), perhaps through the advection of heat by moving liquid columns.

The concentrated and dilute liquids on either side of the phase boundary may be thought of as two sides of a U-tube, connected at the top through the still-condenser line. In this U-tube there are three fluid interfaces (in the still, condenser, and mixing chamber) that may translate in response to changes in the viscous pressure drop across the still line or hydrostatic pressures. This connection between hydrostatic pressure and moving liquid columns may help to explain the dependence of the mixing chamber temperature upon tilt and azimuthal angles.

## ACKNOWLEDGMENTS

We thank Johanna Nagy and Henric Krawczynski of Washington University in St. Louis for allowing us to borrow the dilution refrigerator. We also thank Vincent Kotsubo of NIST and Gregory Swift of Swift Science and Engineering for discussion and leadership. Contribution of NIST, not subject to copyright. R.S. and S.B. acknowledge support from the Professional Research Experience Program (PREP) between the University of Colorado Boulder and NIST under award number 70NANB18H006. Figures were generated using Matplotlib.

## REFERENCES

1. V.S. Edel'man, "A dilution refrigerator with condensation pump," *Cryogenics*, vol. 12, no. 5, Oct. 1972, doi: 10.1016/0011-2275(72)90114-2, pp. 385–387.
2. V.A. Mikheev, P.G. Noonan, A.J. Adams, R.W. Bateman, and T.J. Foster, "A completely self-contained cryogen-free dilution refrigerator, the TritonDRTM," *Low Temp. Phys.*, vol. 34, no. 4, Apr. 2008, doi: 10.1063/1.2911663, pp. 404–408.
3. G. Teleberg, S.T. Chase, and L. Piccirillo, "A Cryogen-Free Miniature Dilution Refrigerator for Low-Temperature Detector Applications," *J. Low Temp. Phys.*, vol. 151, no. 3, May 2008, doi: 10.1007/s10909-008-9724-7, pp. 669–674.
4. S.T. Chase, T.L.R. Brien, S.M. Doyle, and L.C. Kenny, "Pre-cooling a 3He/4He dilutor module with a sealed closed-cycle continuous cooler," *IOP Conf. Ser. Mater. Sci. Eng.*, vol. 502, Apr. 2019, doi: 10.1088/1757-899X/502/1/012134, p. 012134.
5. R. Radebaugh, *Thermodynamic Properties of He3-He4 Solutions with Applications to the He3-He4 Dilution Refrigerator*. NBS Technical Note 362, United States Department of Commerce (1967), Available: <https://nvlpubs.nist.gov/nistpubs/Legacy/TN/nbstechnicalnote362.pdf>
6. F. Pobell, *Matter and Methods at Low Temperatures*, 3rd ed. Berlin Heidelberg: Springer-Verlag (2007), Accessed: Dec. 28, 2018. Available: [www.springer.com/us/book/9783540463566](http://www.springer.com/us/book/9783540463566)
7. Y.H. Huang, G.B. Chen, and V.D. Arp, *Helium-3 Thermophysical Properties Program – He3Pak, Version 2.0*. Horizon Technologies, Littleton, CO, USA (2009). Available: <https://htess.com>